PROCEEDINGS OF SPIE

SPIEDigitalLibrary.org/conference-proceedings-of-spie

Outlier analysis for understanding process variations and probable defects

Mihir Gupta, Paulina Rincon Delgadillo, Hyo Seon Suh, Sandip Halder, Mircea Dusa

Mihir Gupta, Paulina Rincon Delgadillo, Hyo Seon Suh, Sandip Halder, Mircea Dusa, "Outlier analysis for understanding process variations and probable defects," Proc. SPIE 12053, Metrology, Inspection, and Process Control XXXVI, 120530Q (26 May 2022); doi: 10.1117/12.2616679

SPIE.

Event: SPIE Advanced Lithography + Patterning, 2022, San Jose, California, United States

Outlier analysis for understanding process variations and probable defects

Mihir Gupta, Paulina Rincon Delgadillo, Hyo Seon Suh, Sandip Halder, Mircea Dusa
imec, Kapeldreef 75, 3001 Leuven, Belgium
mihir.gupta@imec.be

ABSTRACT

To understand extreme ultraviolet (EUV) lithography performance of various materials (resists, underlayers etc) or processes (bake, development etc.) in terms of process window (PW) and defectivity, we typically use e-beam based tools (e.g., CDSEM) or optical inspection and defect reviews. The optical inspections can scan large areas quickly to pick up potential defects but give little information about the defect's morphology. The e-beam inspections provide us with metrology information (CD, PW etc.) and detailed defect characteristics, but is very slow. To connect this gap, i.e., to be able to make high-level projections about process window variations and probable defectivity while scanning small area quickly, we need an intermediate analysis methodology bridging optical inspection and CDSEM analysis. With this objective, we present a new data analysis methodology for understanding process variations and probabilities of developing defects, by performing statistical analysis of the local CD variations for line/spaces patterned using EUV lithography. The local CDs obtained from a CDSEM image are assumed to follow the normal distribution curve. The deviations from the distribution i.e., the outlier local CD data, represent potential bridge and break defects and can help identify the probabilities of obtaining these defects for a process, material, condition etc. The outlier counts are obtained by performing statistical hypothesis testing (e.g., generalized extreme studentized deviate test) of the local CDs. Additional metrics such as p-value of the Shapiro-Wilk hypothesis test for local CD distribution are also measured to quantify the degree of normality of the distribution. Using these metrics, we compared different resists, underlayers and L/S pitches to demonstrate the novel utility of this data analysis method in understanding process variations and finding probable defects. We also demonstrate the validity of this analysis method by correlating the obtained outlier count with the standardized line roughness measurements and defectivity counts.

Keywords: EUV, lithography, metrology, statistics, defects, process window

1. INTRODUCTION

With the progression of the Moore's law, the scaling down of critical dimension (CD) for lithography is accompanied by challenges in metrology and data analysis. We need faster turnaround times, better metrology techniques and novel ways to interpret the data. A typical way of working to analyse process window post-lithography is using e-beam based tool such as CDSEM to image the patterns for each input condition and construct a process window based on mean parameters extracted from each SEM image. This method of analysis has been very useful in centring the lithography input parameters to obtain an optimize process. A drawback of this way of analysis is that it gives a binary view of the process parameters and misses out on subtle variations and spreads impacting the output variable, e.g., line CD. Another method of analysing processes or materials is by doing a defectivity analysis (post lithography or post etch) using only e-beam inspection or optical inspection followed by defect review. E-beam inspection method scans very small wafer area and is very slow compared to optical inspection, but give much more details about the defects, while optical inspection although fast and scan large areas, does not provide information of the defect morphology.

In this paper, we present a new method to analyse process window space and the probability of developing defects by statistically analysing local CDs obtained from CDSEM images. This method offers a trade-off between typical CDSEM based inspection and optical inspection, by offering quick process window space analysis and offering projections for defectivity as well. The local CDs from a SEM image are assumed to follow normal distribution, and the outlier CDs from that distribution are detected. These outlier CD represent potential bridges and breaks (Figure 1) and help identify the probabilities of obtaining defects for a specific process, material, condition etc. Additionally, we also evaluate the degree of normality of local CD distribution with change in target CD. This helps in pin-pointing the optimum L/S CD where the process is most normally distributed, and therefore, offers minimum outliers.

Metrology, Inspection, and Process Control XXXVI, edited by John C. Robinson, Matthew J. Sendelbach,
Proc. of SPIE Vol. 12053, 120530Q · © 2022 SPIE · 0277-786X · doi: 10.1117/12.2616679

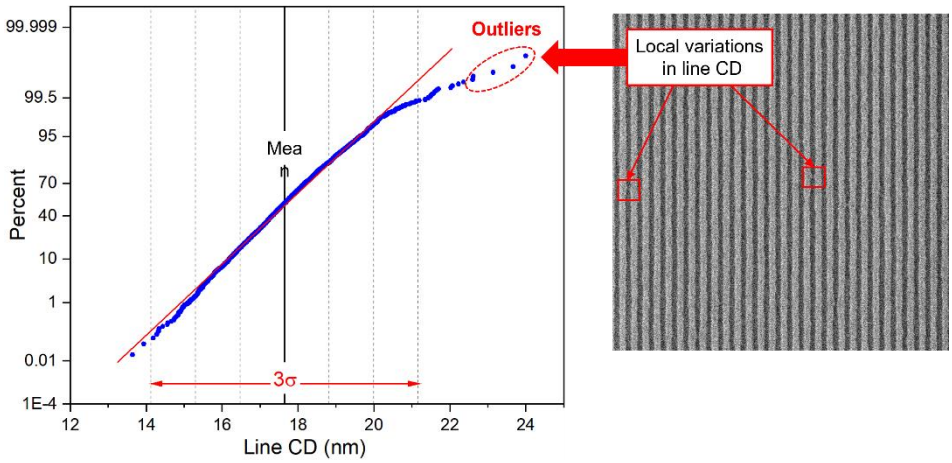

Figure 1: Outliers detected for a local CD distribution, corresponding to variations in the line CD

2. OUTLIER ANALYSIS METHODOLOGY

To understand variations in process defect window, we used a focus-exposure matrix (FEM) wafer. In this paper, we are discussing line-space (L/S) structures with a pitch of 32 nm and 28 nm for after development inspection (ADI) with CDSEM CG6300. After EUV exposure on NXE3400 and development, we used CDSEM to take 1 image per die for the entire FEM wafer. The pixel size for the SEM image is approximately 0.8 nm per pixel.

This analysis of the extraction of local CDs to quantify the outlier and the normality of the local CD distribution and in turn assessing process variations and probable defects includes the following steps:

2.1 Extracting local CD

The extraction of local CD was done by selecting a specific length of line segment window, in this paper, 5 pixels in y-direction, resulting in a line segment window of about 4 nm length. The line CD (along the x-direction) was then measured for these 5-pixel window along the whole line and for the full image as shown in Figure 2. This set of local CDs for the full image (approximately 4500 CDs) per field of view were taken as one set of local CD data. The local CD extraction in this way was carried out for all the images of the FEM wafer.

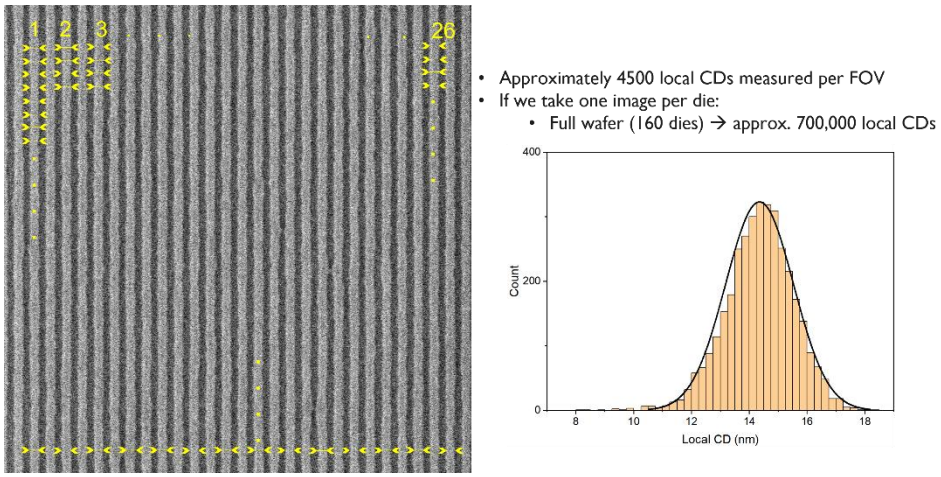

Figure 2: Extraction of local CDs from a SEM image by selecting a 'line segment window' of 4 nm (5 pixels in y-direction) and plotting the histogram to obtain a normally distributed bell curve.

2.2 Finding outliers and quantifying the degree of normality of the local CD distribution

Each CDSEM image i.e., each local CD data set is then analysed to find how many local CDs are deviating from the assumed normal distribution (Figure 1), which can help in understanding local CD variations and their contribution to process and defect window.

The quantification of outlier was done using the standard generalized extreme studentized deviate test (ESD) [1], [2] to detect outliers for each local CD distribution, as shown in Figure 1Figure 1. For each SEM image, i.e., for each CD data set, we can then also calculate the number of outliers found per mm of line length, which is a metric that can be used for comparing materials, processes etc.

In addition to calculating the number of outliers per image or condition, we also quantified the degree of normality of the local CD distribution. This was done performing hypothesis tests (e.g., Shapiro-Wilk test [3], [4]) to find p-value for the normality of a given local CD dataset, as shown in Figure 3. The p-value is calculated for each local CD dataset (each image/condition) which tells us the degree of normality for each data set. The p-value gives us the quantification of how strongly a data is close to an ideal normal distribution, so a higher p-value indicated stronger evidence for normality. This calculated p-value can then be plotted against the mean CD for each dataset/image as shown in Figure 3. In this way we can compare how the curve of the data points in a p-value plot (Figure 3) change with materials and processes to find the optimum CD for centring a process or to compare the width and spread of process window, discussed further in section '3. Application and discussion'. Additionally, we can also set an arbitrary threshold (in this paper, p-value ≥ 0.05), to quantify number or the percentage of dies/images that show the expected normal distribution, in Figure 3, that would be all the data point above the red dashed line at p-value = 0.05 (i.e., data points with p-value ≥ 0.05).

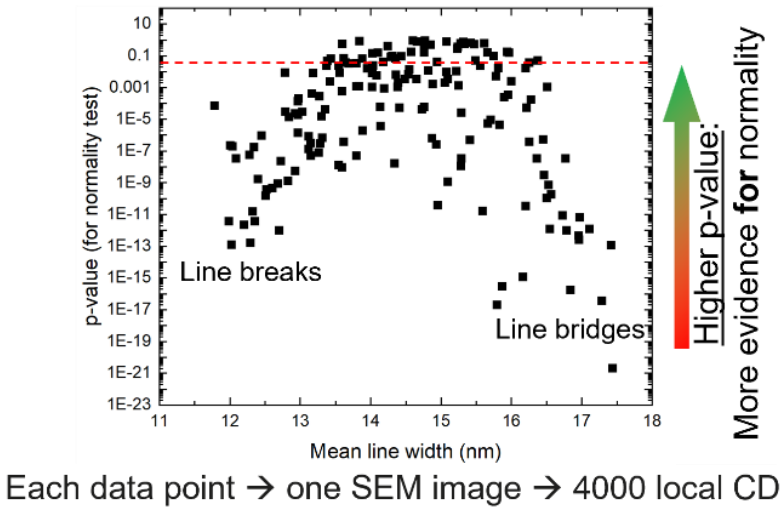

Figure 3: p-value extracted from multiple local CD datasets indicating the variation in the degree of normality with respect to change in mean line width. A higher p-value implies that there is stronger evidence for normality and therefore is desirable. This plot shows that the optimum line CD for highest degree of normality occurs between 14 to 15 nm line CD.

The p-value plot shows us how the normality of local CD distribution changes with mean CD which is defined by dose and focus settings. This distribution of p-value with mean CD will change for each process material and is a useful tool for understanding how large the process window is. A smaller p-value indicates a larger deviation from an ideal normal distribution while a higher p-value indicates a smaller deviation from an ideal normal distribution.

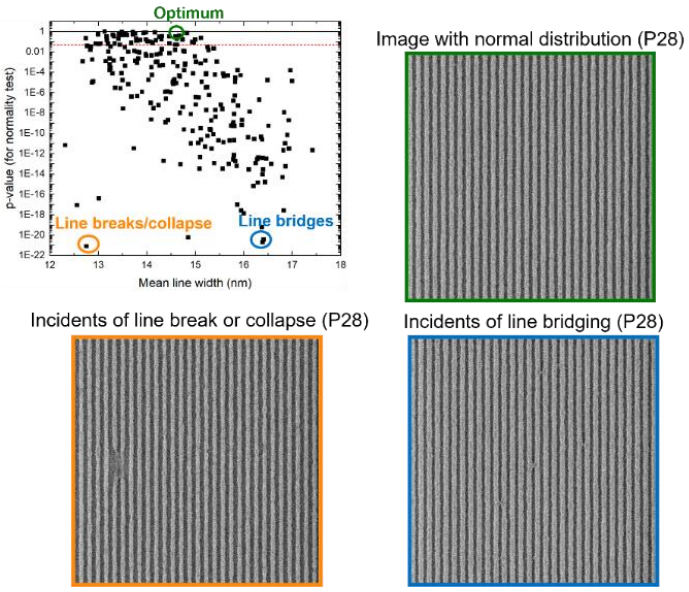

Figure 4: CDSEM images for extreme p-value points showing best (green) and worst conditions (orange: breaks/collapse and blue: bridges)

As can be seen from Figure 4Figure 3, the p-value of images on the extreme CD range (12 to 13 nm and 16 to 17 nm) is lower than in the centre around 13 to 14 nm, which indicates the extent possibility of developing line bridges or breaks at the extreme CD values, while optimum performance at around 13 to 14 nm line CD. This CD window for optimum performance will change from material to material and process to process as discussed in the next section.

3. APPLICATION AND DISCUSSION

We applied the outlier analysis methodology to various cases, including resist comparison for two different L/S pitches, impact of resist film thickness, and for comparing two different underlayers (ULs). To benchmark this novel analysis methodology to the existing metrics, we correlated the results with line roughness and ADI defectivity data obtained using traditional methods.

3.1 Comparing photoresists for P32 and P28 nm line/space

We compared 3 different resists for the normality vs line width analysis, for P32 L/S as shown in Figure 6 and for P28 L/S as shown in Figure 6Figure 6.

For P32 L/S (Figure 6), we see that resist_3 shows maximum data points close to or above the threshold of p-value of 0.05 compared to resist_1 and resist_2. This indicates that within the CD range of 15 to 17 nm, resist_3 has most data points that exhibit a stronger normal distribution compared to resist _1 and resist_2, which in turn indicates better performance within that CD range, a larger process window and a smaller number of outliers.

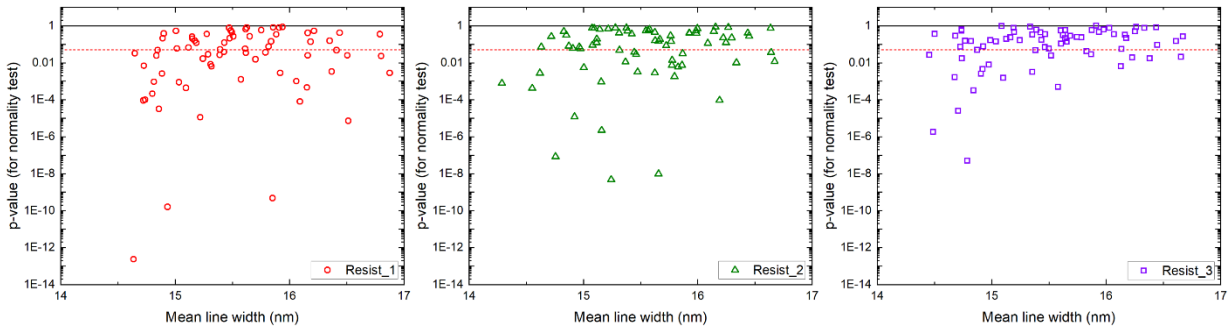

Figure 5: Comparing resists for P32 nm using normality test for datasets with different line CDs (each data point represents one SEM image).

For P28 L/S (Figure 6), with change in line CD, resist_1 shows least change in p-value (minimum slope of line fit), while resist_2 shows maximum change in p-value with change in line width (steeper slope). This indicates that resist_1 is lease sensitive to line width variation, as is for a specific line CD e.g., 15 nm, we can expect CD distribution to have repeatedly better normal distribution compared to resist_2. However, resist_3 shows maximum number of datapoints for p-value > 0.05 (red dotted line), indicating that resist_2 will show highest number of normally distributed local CD data sets for the CD window 13 nm to 15 nm.

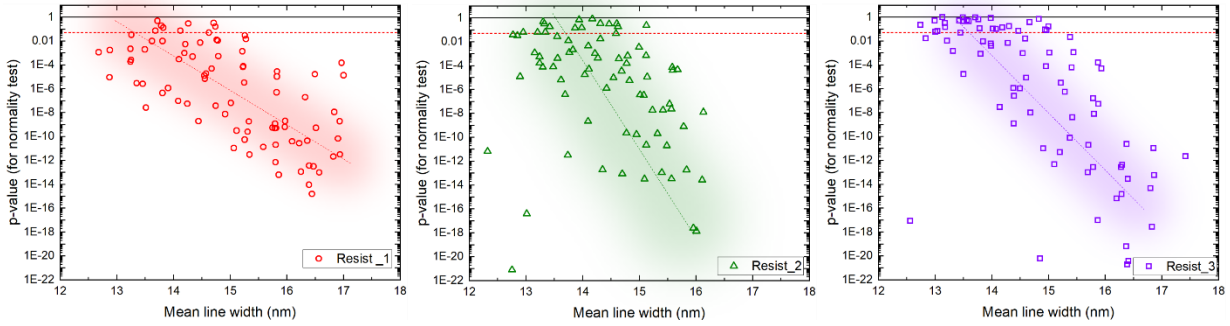

Figure 6: Comparing resists for P28 nm using normality test for datasets with different line CDs (each data point represents one SEM image).

We can also look at P28 and P32 together in the same plot for the 3 resists, as shown in Figure 7. Here, we are plotting p-value versus trench CD (instead of line CD) for the convenience of visuals in the graphs, and the same plot for line CD will give the same result. Here, we can clearly see that for all the three resists, P32 data points are much closer the threshold value compared to P28, because P32 is a much more mature process, and we can expect better performance compare to the still under development P28 structures.

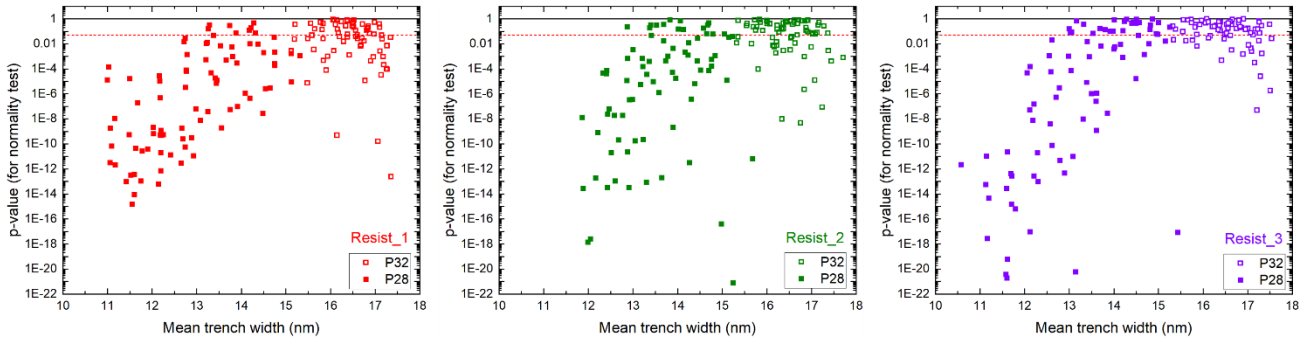

Figure 7: Comparing pitch 28 nm and 32 nm for the 3 resists for p-value plot vs space/trench CD width (each data point represents one SEM image).

3.2 Comparing resist thickness

As we move towards the high-NA EUV lithography, we expect the resist thickness to reduce because of reduced depth of focus (DOF). This will result in changes in the lithography printing performance, and we can characterize this with outlier analysis. In Figure 8, we show a comparison of 30 nm versus 35 nm resist film thickness for P28 L/S structures. Here, we try to separate the 2 graphs into two CD regimes (I and II) splitting at half-pitch CD 14 nm. If we compare 30 nm versus 35 nm resist film thickness for CD regime II, we do not see any major difference, as we see a very similar spread of the local CD datasets. However, if we reduce the line CD to less than 14 nm and compare CD regime I, we see a clear difference, where 30 nm film thickness gives higher number of normally distributed data points compared to 35 nm, as for 35 nm film thickness, we see a larger vertical spread with data points at lower p-value. This indicates that resist thickness makes a difference only if a process wants to target narrower line CD (less than 14 nm for P28 nm). This is a consequence of high aspect ratio of the resist lines at narrower CD, resulting in more collapse when the line CD reduces. If the line CD is wider, i.e., lower aspect ratio and better footing, we do not see collapses and the performance of both 30 nm and 35 nm film thickness is similar in CD regime II.

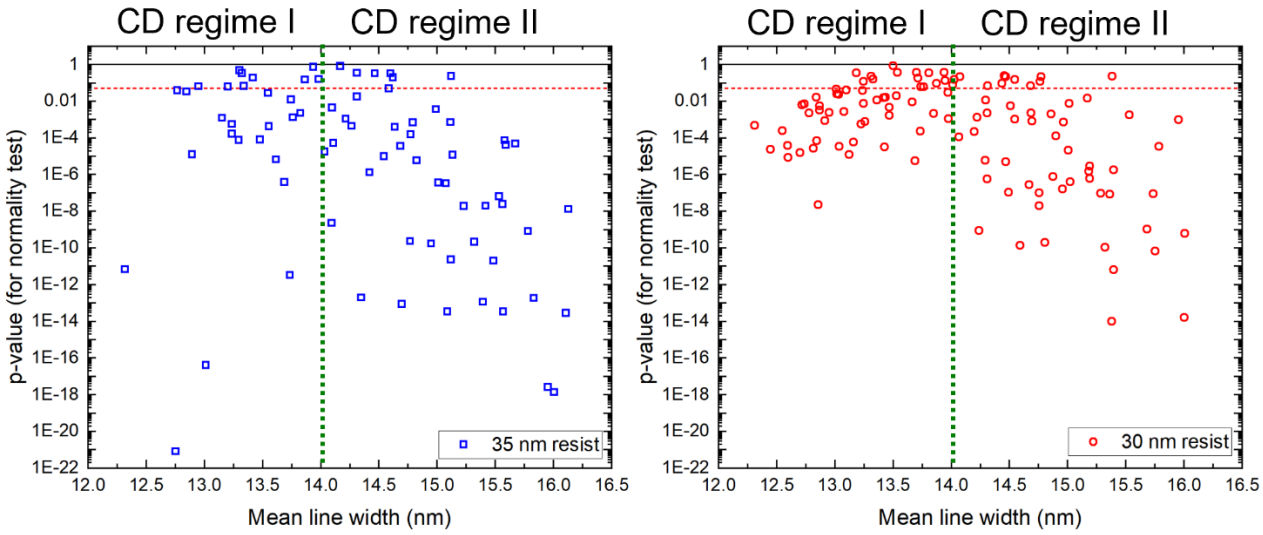

Figure 8: Resist film thickness comparison for P28 L/S structures (each data point represents one SEM image).

3.3 Comparing different underlayers

We compared 2 underlayers for P28 L/S structures using both normality test as well as outlier quantification, as shown in Figure 9. We observe a clear difference in the 'minimum outlier process window' which can be confirmed by both the tests. UL_2 shows larger CD window that offers higher p-value as well as lowest incidents of outliers/mm line length. For the p-value plot, we are typically looking at horizontal spread when comparing materials or processes, but the vertical spread of p-value at a specific CD is equally important. If we look at line CD 12.5 nm in the p-value plot, we can see that UL_1 gives a much larger vertical spread compared to UL_2, indicating that with UL_1, the chance of obtaining a normally distributed local CD is lower compared to UL_2, which has a tighter vertical spread.

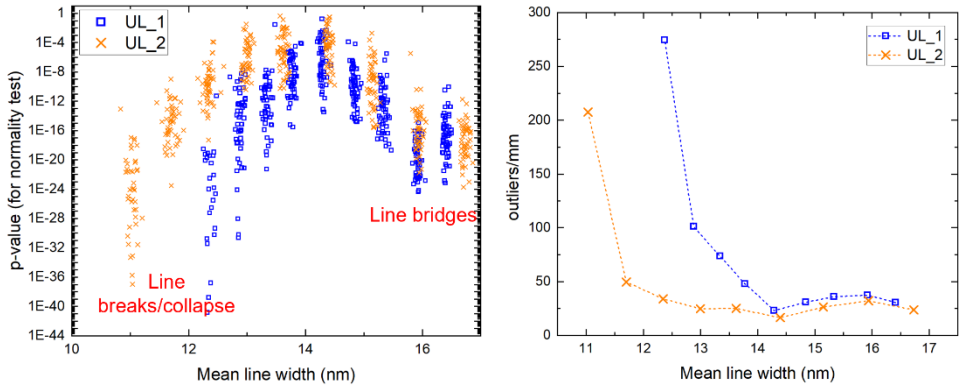

Figure 9: Comparing underlayers using normality test and outlier test for datasets with different line CDs (each data point represents one SEM image).

3.4 Correlation with defectivity and line roughness measurements

To correlate and benchmark these new metrics (e.g., outliers/mm line length) with more commonly used metrics such as line roughness or traditional defectivity analysis, we compared the detected outliers/mm line length with standard ADI defectivity analysis (Figure 10) and also with unbiased LER and LWR as shown in Figure 11Figure 11. We see a clear correlation with defectivity (Figure 10) as with reduction in line CD we start to see line collapses earlier for UL_1 than for UL_2, which is the same result we obtain in the outlier/mm line length plot where outlier count for UL_1 starts to increase earlier than for UL_2 as we reduce line CD. We also compared with unbiased LER and LWR (Figure 11) and here as well we see a clear correlation; as the incidents of outliers/mm line length increase, the LWR as well as LER value also increases.

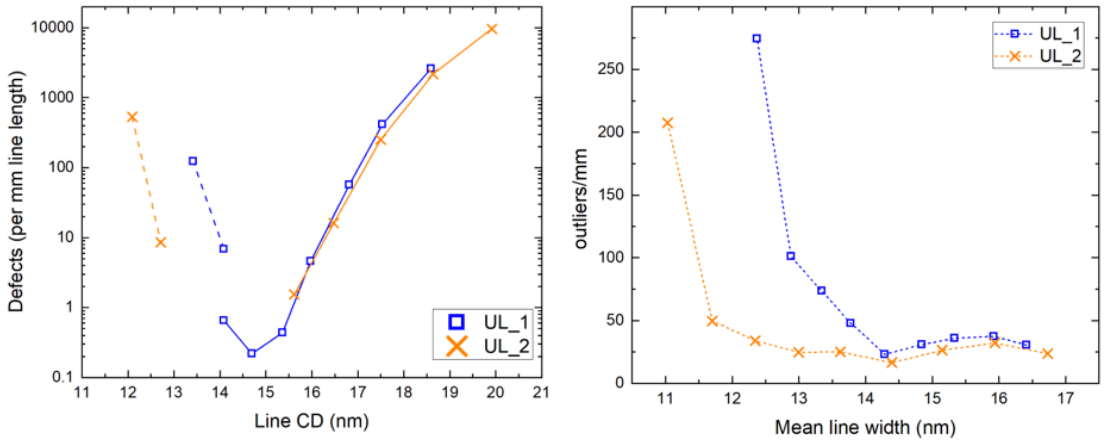

Figure 10: Correlating standard ADI defectivity analysis with outliers/mm line length for 2 different ULs.

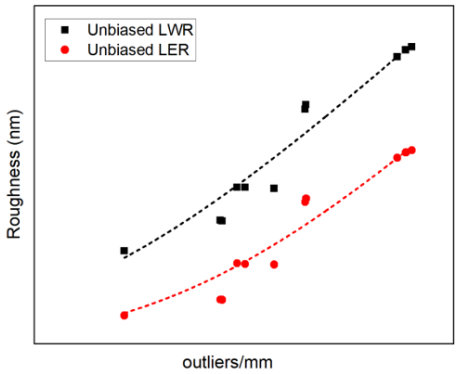

Figure 11: Correlating outliers/mm with unbiased line width and edge roughness

4. CONCLUSION AND OUTLOOK

In this paper we presented a novel analysis methodology for CDSEM images by looking at the statistical analysis of the local CD distribution and quantifying the number of outlier and the degree of normality of the local CD distribution. The outlier analysis of the local CDs offers detailed insights into the variations taking place at localized level and offers a new way to statistically understand process induced or material dependent variations. We presented application cases for various material comparisons and physical parameters, to understand the practical use of such analysis. We also benchmarked this novel analysis to the existing standard metrics such as ADI defectivity (defect per mm line length) and unbiased LWR and LER, and we see a clear correlation, which further strengthens the conclusions obtained from this analysis.

The outlier analysis is ideal for early-stage material/process development and for quick screening of new material chemistries and process parameters, as it does not require additional CDSEM metrology than just 1 image per die/conditions, which is a standard measurement needed after lithography. Hence, this analysis uses existing image data to provide much more information than typical metrics like mean CD, LCDU etc. Additionally, it can also be very useful for understanding line break defects, where traditional after etch inspection (AEI) using optical measurements (e.g., broad band plasma inspections) offer limited sensitivity. Currently, the outlier analysis offers a bridge between initial CDSEM metrology after lithography and final AEI defectivity analysis and is therefore not a substitute for the standard large-scale AEI defectivity. As an outlook, this analysis can be further extended to AEI analysis and after a correlation can be established for large scale AEI defectivity with ADI inspections, which will be very useful in minimizing the effort needed to obtain AEI defectivity.

REFERENCES

[1] B. Rosner, “Percentage points for a generalized esd many-outlier procedure,” Technometrics, vol. 25, no. 2, pp. 165–172, May 1983, doi: 10.1080/00401706.1983.10487848.

[2] NIST, “Generalized ESD Test for Outliers,” *NIST/SEMATECH e-Handbook of Statistical Methods*. https://www.itl.nist.gov/div898/handbook/eda/section3/eda35h3.htm

[3] Shapiro, S. S. and Wilk, M. B. (1965). "An analysis of variance test for normality (complete samples)", Biometrika, 52, 3 and 4, pages 591-611.

[4] NIST, “Anderson-Darling and Shapiro-Wilk tests,” Eng. Stat. Handb., [Online]. Available: https://www.itl.nist.gov/div898/handbook/prc/section2/prc213.htm